Jurnal Teknologi

Full Paper

CAPTURING GREENHOUSE GAS CARBON DIOXIDE TO FORM CARBONATE COMPOUNDS

Wan Nor Roslam Wan Isahak[a*], Zatil Amali Che Ramli[a], Wan Zurina Samad[b], Mohd Ambar Yarmo[b]

[a]Department of Chemical and Process Engineering, Faculty of Engineering and Built Environment, 43600 UKM Bangi, Malaysia.
[b]School of Chemical Sciences and Food Technology, Faculty of Science and Technology, 43600 UKM Bangi, Malaysia.

Article history
Received
15 July 2015
Received in revised form
1 October 2015
Accepted
25 October 2015

*Corresponding author
wannorroslam@ukm.edu.my

Graphical abstract

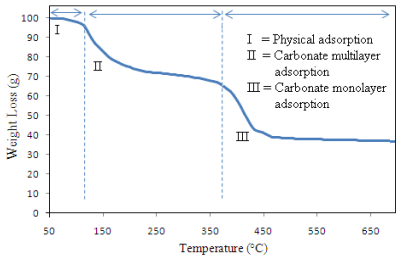

Abstract

The application of CuO and MgO nanoparticles in CO_2 capture was evaluated experimentally using 5% CO_2 in nitrogen via physisorption and chemisorption instrumentation. The structural and surface micrograph of the CuO and MgO nanoparticles were characterized by XRD and TEM, respectively. After CO_2 capture by the CuO nanoparticles, the amounts of oxide, hydroxide, and carbonate phases in the adsorbents were determined by XPS measurements. No hydroxide phase was detected in the MgO nanoparticles because of the efficient transformation of MgO into $MgCO_3$. Monolayer adsorptions of CO_2 were shown to occur in the MgO nanoparticles with a total chemisorption of 5.0 mmol/g. After the fifth cycle, only 3% reduction of the CO_2 chemisorption was reported because of some agglomeration by sintering during desorption.

Keywords: CO_2 capture; nanoparticles; thermodynamic consideration; physical and chemical interactions; carbonates

Abstrak

Penggunaan bahan zarah nano CuO dan MgO dalam penangkapan gas CO2 dikaji menggunakan campuran 5% gas CO2 dalam nitrogen melalui peralatan *physisorption* dan *chemisorption*. Struktur micrograf dan permukaan zarah nano CuO dan MgO, masing-masing telah diciri menggunakan XRD dan TEM. Selepas jerapan gas CO2 oleh zarah nano CuO, sejumlah logam oksida, hidroksida dan karbonat telah terbentuk dan ditentukan oleh alatan XPS. Fasa Hidroksida tidak dikesan dalam MgO berzarah nano kerana pembentukan yang efisien kepada sebatian MgCO3. Jerapan lapisan tunggal gas CO2 telah terbukti berlaku pada sistem MgO dengan sejumlah 5.0 mmol/g jerapan kimia telah berlaku. Selepas kitaran kelima, terdapat hanya 3% pengurangan kapasiti jerapan kimia gas CO2 dilaporkan.

Kata kunci: Penangkapan gas CO_2; zarah nano; pertimbangan termodinamik; interaksi fizikal dan kimia; karbonat.

1.0 INTRODUCTION

CO_2 is considered to be a major greenhouse gas (GHG) contributing to global warming. Since 1850, the average atmospheric concentration of CO_2 has increased from 280 to 370 ppm; as a result, the average global temperature has increased by 0.6–1 °C [1]. The International Panel on Climate Change

(IPCC) predicts that by the year 2100, the atmosphere may contain up to 570 ppm of CO_2, causing a rise in the mean global temperature of ~1.9 °C [2]. The Annual Energy Outlook 2013 (AEO2013), prepared by the U.S. Energy Information Administration (EIA), reported CO_2 emissions of 17.5 ton per person for 2011 [3].

Commonly, charcoal or carbon materials with a porous structure such as activated carbons and microporous amorphous carbon materials are widely used as CO_2 adsorbents [4-7]. Previous studies showed that the adsorption of CO_2 by calcium oxide (CaO) and magnesium oxide (MgO) is high at 550 and 150–400 °C, respectively [8]. $CaCO_3$ requires very high energy to decompose into CaO and CO_2 as a recovery method of CO_2 before transforming it to other valuable products such as fuel and chemicals (calculation under standard conditions: pressure for each product and reactant, 1 atm; temperature, 298 K). However, these conditions increase the production cost and lead to a less efficient recycling.

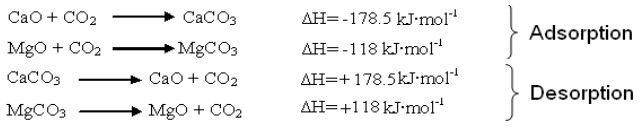

CO_2 molecules are usually soft acids [9,10]. This fact indicates that the presence of strongly basic phases such as oxides can enhance the carbon dioxide adsorption capacity. Modification of a bulky oxide into a smaller nanoparticle can increase its reactivity to CO_2 molecules. Several oxide materials have been applied as superior adsorbents such as nano-potassium carbonate mixed MgO [11,12], Fe_2O_3, γ-Al_2O_3, and TiO_2 nanoparticles [13], and nano-Zr in metal-organic frameworks (MOFs) with amine functional groups [14]. In other works reported by Baltrusaitis & Grassian [15], oxide metal hydroxylated nanoparticles showed good sorption behavior in dry conditions. There is an adsorbed layer of water on iron (III) oxide surfaces, which plays a part in understanding the surface chemistry of CO_2 adsorption. However, the real mechanism of interaction of CO_2-metal oxide surfaces at low temperature has not yet been fully explained [12].

Kim et al. [16] reported a study on CO_2 adsorption using copper (I) oxide (Cu_2O) on porous carbons. The porous carbon with a high specific surface area accelerates the CO_2 adsorption ability of Cu_2O at room temperature. However, in our previous study, the CuO adsorbent shows a better adsorption ability compared with that of the copper oxide with a lower oxidation number (Cu_2O). The better basicity, porosity, and morphology are considered the properties that allow CO_2 to be adsorbed at a higher level [17].

This work aims to synthesize and study the properties and performance of nanoparticle adsorbents based on CuO and MgO for CO_2 capture. The potential of CuO and MgO for CO_2 adsorption and desorption was determined by a simple thermodynamic consideration. The adsorption studies of CO_2 using copper oxide (CuO) and magnesium oxide (MgO) nanoparticles were performed at room temperature. Furthermore, the effect of particle size was studied comprehensively. Complete characterization was carried out for a better understanding of CO_2 physisorption and chemisorption on the CuO and MgO nanoparticle surfaces. The CO_2 desorption and regeneration ability of the potential adsorbents was also studied.

2.0 EXPERIMENTAL

2.1 Thermodynamic Approach

The CO_2 adsorption characteristics of several potential metal oxides such as CuO and MgO were determined by thermodynamic calculations, in particular the chemisorption to form carbonate compounds. Any consideration of various materials as CO_2 adsorbents must take into account their chemical properties. A thermodynamic approach will provide useful information (data from Wagman et al. [18]) to discuss the issues in terms of the Gibbs-Helmholtz relationship shown below.

$\Delta G = \Delta H - T\Delta S$

If $\Delta G = 0$,

$T = \Delta H/\Delta S$

2.2 Synthesis and Characterization of Adsorbents

The metal oxides were purchased from Aldrich Company. Before being used as adsorbents, the CuO and MgO were heated to 300 °C and 500 °C, respectively, to remove any carbonates.

a) Metal oxides nanoparticles

The CuO and MgO nanoparticles were synthesized using sol gel or wet chemical techniques. First, 5 g each of $Cu(NO_3)_2 \cdot H_2O$ and $Mg(NO_3)_2 \cdot H_2O$ were dissolved in 20 mL of ethanol. The solution was sonicated for 15 min and stirred at 50 °C for 1 h. The solution was left to sit for 1 d for gel formation. The gel was dried and calcined at 400 °C for 3 h.

a) Physical and chemical characterization

The crystallinity analyses of the samples were performed using a Bruker DB-Advance X-ray Diffractometer (XRD), Germany. The analyses were performed with 1-g samples, employing Cu Ka radiation at 2θ ranging from 10° to 80°. The infrared spectra of the adsorbent samples were recorded on a spectrum 400, FT-IR/FT-NIR Spectrometer (Perkin Elmer, UK) using attenuated total reflectance (ATR). For all tests, 0.5 mg samples were used. The surfaces of the nano adsorbents were studied using transmission emission microscopy (TEM). The oxidative mass losses of the samples were analyzed in air using

dynamic thermal gravimetric analysis (TGA) with a simultaneous TGA-DTG system (Model: Mettler Toledo). To reduce the influence of the sample quantity on the analyses, 5±0.2 mg of each sample was used in each analysis, and a constant air flow of 50.0 mL min^{-1} was maintained throughout the entire process. To minimize possible differences in the moisture content between samples, all TGA samples were equilibrated at 50 °C for 5 min before being heated to 700 °C at a ramping rate of 5 °C min^{-1}.

2.3 CO_2 Adsorption

The CO_2 physisorption and chemisorption were measured using CO_2 adsorption isotherm analysis and TPD-CO_2 instrumentation, respectively. A mixture of 5% CO_2 in nitrogen was used in this study. These physisorption and chemisorption studies were performed at 25 and 40 °C, respectively.

3.0 RESULTS AND DISCUSSION

3.1 Thermodynamic Approach

In Table 1, we compare the thermodynamic terms (kJ·mol^{-1}) for several reactions involving MgO and CuO at room temperature. The formation of $MgCO_3$ from MgO and CO_2 is associated with a large negative ΔH (117.5 kJ·mol^{-1}). This process is a spontaneous reaction under standard conditions (1 atm and 298 K) with a value of ΔG of -65.4 kJ·mol^{-1}. However, the reaction between CuO and CO_2 is thermodynamically less favorable, with a ΔG of +4.9 kJ·mol^{-1} under standard conditions.

According to the thermodynamic calculations, $MgCO_3$ began to decompose at 380 °C, where the value of ΔG is greater than zero (+3.2 kJ·mol^{-1}). It was noted that the rate of CO_2 desorption from $MgCO_3$ was increased by heating. Furthermore, the desorption reaction of CO_2 by the decomposition reaction of $CuCO_3$ is favorable at very low temperatures (even at room temperature). However, $CuCO_3$ almost completely decomposed into CuO and CO_2 within the temperature range 290–300 °C. This decomposition was characterized by typically large positive ΔH (+45.5 kJ mol^{-1}) and ΔS (+169 J·mol^{-1}·K^{-1}) values, which meant that some heat was required to break the strong chemical attractions between O=C=O and Cu-O [18,19]. The error involved in the values of thermodynamics data was approximately ±16.7 kJ·mol^{-1}. $CuCO_3$ decomposition to CuO and CO_2 was expected at ~150 °C. However, we noticed that the decomposition of $CuCO_3$ actually occurred at 300 °C

Table 1 Thermodynamics of reactions involving adsorption-desorption of CO_2 at various for different Oxides.

Reaction involved	ΔH (kJ·mol^{-1})	ΔS (J·mol^{-1}·K^{-1})	ΔG (kJ·mol^{-1})	T (K)	Reaction possibility
CuO (s) + CO_2 (g) --> $CuCO_3$ (s) (Adsorption)	-45.5	-169	+4.9	298.0	Favourable
MgO (s) + CO_2 (g) --> $MgCO_3$ (s) (Adsorption)	- 117.5	- 175	- 65.4	298.0	Favourable (Reaction spontaneous)
$CuCO_3$ --> CuO + CO_2 (Desorption- Route 1)	+45.5	+169	-4.9	298.0	Favourable (very low temperature)
2 $CuCO_3$ (s) --> Cu_2O (s) + 2 CO_2 (g) + ½ O_2 (g) (Desorption- Route 2)	+233.0	+447.6	-4.2	530.0	Favourable (high temperature)
$MgCO_3$ (s) --> MgO (s) + CO_2 (g) (Desorption)	+117.5	+175	+ 3.2	653	Favourable at 653 K

3.2 Crystallinity Properties

XRD analyses were performed for the CuO bulk and nanoparticles before and after CO_2 adsorption. Fig. 1 (a) shows the clear changes of CuO into $CuCO_3$. The XRD pattern of CuO, which consists of a monoclinic 1176). However, a small amount of carbonate intermediate is detected in the MgO after CO_2 exposure as peaks at approximately 19.1°, 51.5°, and 58.2°, which are assigned to the planes of $Mg(OH)_2$ (JCPDS 75-1527). It was noted that the oxide was changed to the hydroxide after reacting with moisture to accelerate the formation of carbonates. The MgO was fully converted into carbonates after 6 h of CO_2 adsorption. The observed $MgCO_3$ diffraction peaks are in good agreement with those of the JCPDS card (JCPDS 88-1802).

structure, and the diffraction data match very well with the JCPDS card of CuO (JCPDS 80-1268). The XRD pattern (Fig. 1 (b)) of the catalysts obtained is identical to that of single-phase MgO with a cubic structure, and the diffraction data are in good agreement with the JCPDS card of MgO (JCPDS 71-

Table 2 gives the crystallite properties of the CuO and MgO bulk and nanoparticles before and after CO_2 adsorption. The atomic composition of MgO changed from Mg (60.3 wt%) and O (39.7 wt%) to Mg (42.2 wt%), O (49.5 wt%), and C (8.3 wt%) after 1 h of

CO_2 adsorption. The O and C components were increased to 56.9 and 14.2 wt%, respectively, after 6 h of adsorption. The CuO nanoparticles also showed the same pattern of increase in the O and C (wt%) concentrations (Table 2).

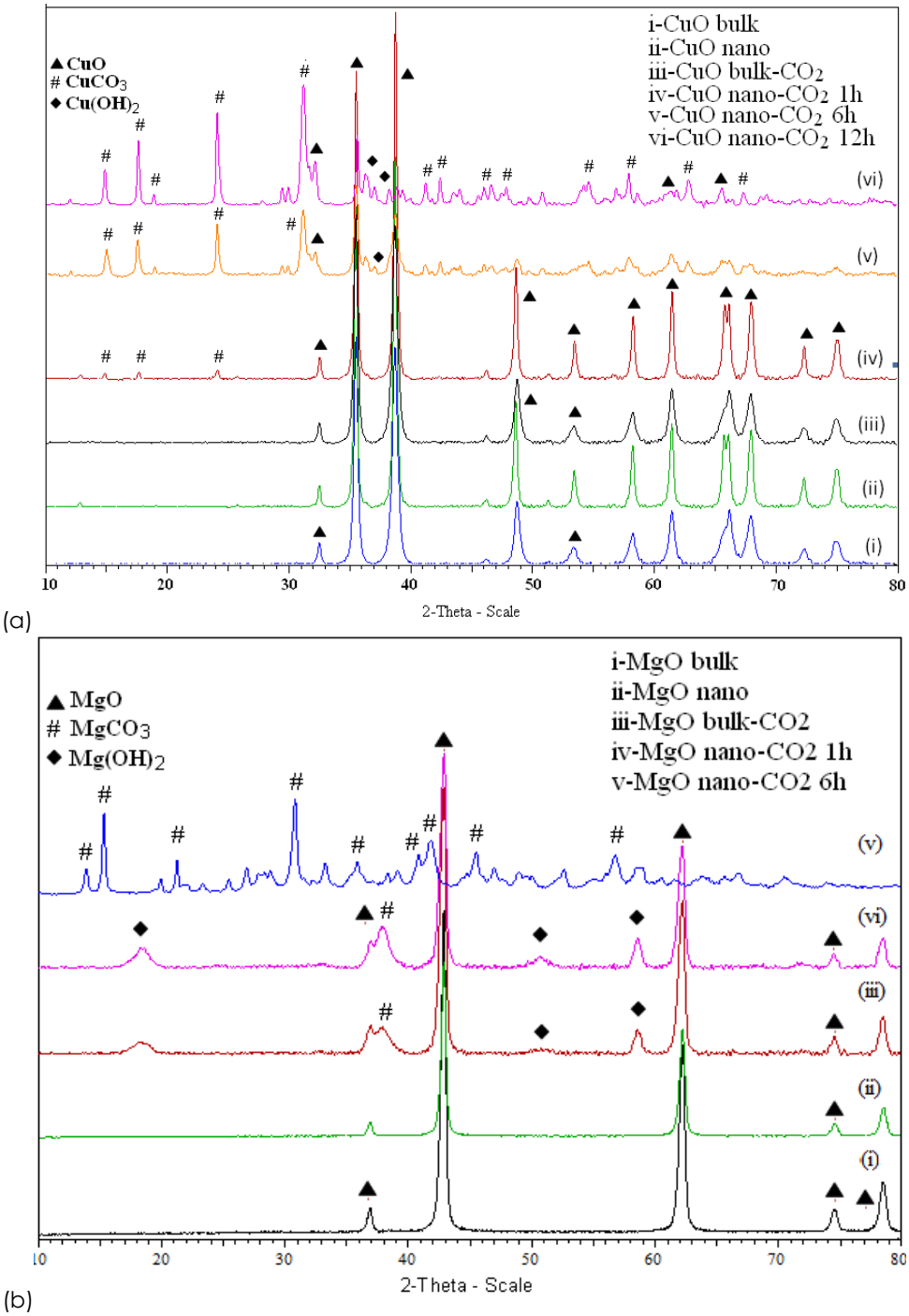

Figure 1 XRD diffractogram of CuO and MgO, before and after CO_2 exposure

Table 2 Crystallites size, lattice system and composition of adsorbents

Compounds	Lattice system	Crystallite size (nm) (by Scherrer equation)	Compositions (wt.%)		
MgO	Cubic	24.4	Mg/Cu (%)	O (%)	C (%)
MgO	Cubic	24.4	60.3	39.7	n.d
CuO	Monoclinic	32.7	79.9	20.1	n.d
MgO nano	Cubic	10.9	60.3	39.7	n.d
MgO nano- 1 h (CO_2)	Cubic	14.2	42.2	49.5	8.3
MgO nano- 6 h (CO_2)	Cubic	16.2	28.8	56.9	14.2
CuO nano	Monoclinic	24.0	79.9	20.1	
CuO nano- 6 h (CO_2)	Monoclinic	18.0	60.3	30.8	8.9
CuO nano- 12 h (CO_2)	Monoclinic	9.3	60.3%	28.6	11.1

Note: n.d. is corresponding to not detect.

3.3 Fourier Transform Infrared Spectroscopy (FT-IR) Study

From Fig. 2, FTIR experiments show distinguishable carbonate species adsorbed on different planes and defects, vibrating in different IR frequency ranges. For example, non-coordinated carbonate was observed at 1410 cm^{-1}, while monodentate carbonates were detected in the range 1130–770 cm^{-1} [20-23]. For bulk MgO after CO_2 saturation, some $Mg(OH)_2$ or moisture was detected at ~3700 cm^{-1}. This may be the result of moisture from the CO_2 source reacting with the highly hygroscopic mesoporous MgO. The new, higher intensity peaks for MgO nanoparticles in Fig. 2 (a)(iv) show improved carbonate formation with a clear spectra compared to the fresh bulk MgO (Fig. 2 (a)(ii)). This indicates that the higher surface area and structure of the MgO nanoparticles can increase the mobility and CO_2-metal surface interaction for better adsorption.

Eight significant bands were identified (Fig. 2 (b)(ii)). The band at 3370 cm^{-1} represents the O-H group of the $Cu(OH)_2$ phase. This data is in agreement with the XRD shown in Fig. 1 (b). Other bands represent monodentate CO_3 at 1497, 1105, 1048, and 819 cm^{-1}; bidentate CO_3 at 887 and 755 cm^{-1}, and non-coordinated CO_3 at 1410 cm^{-1} [22,23].

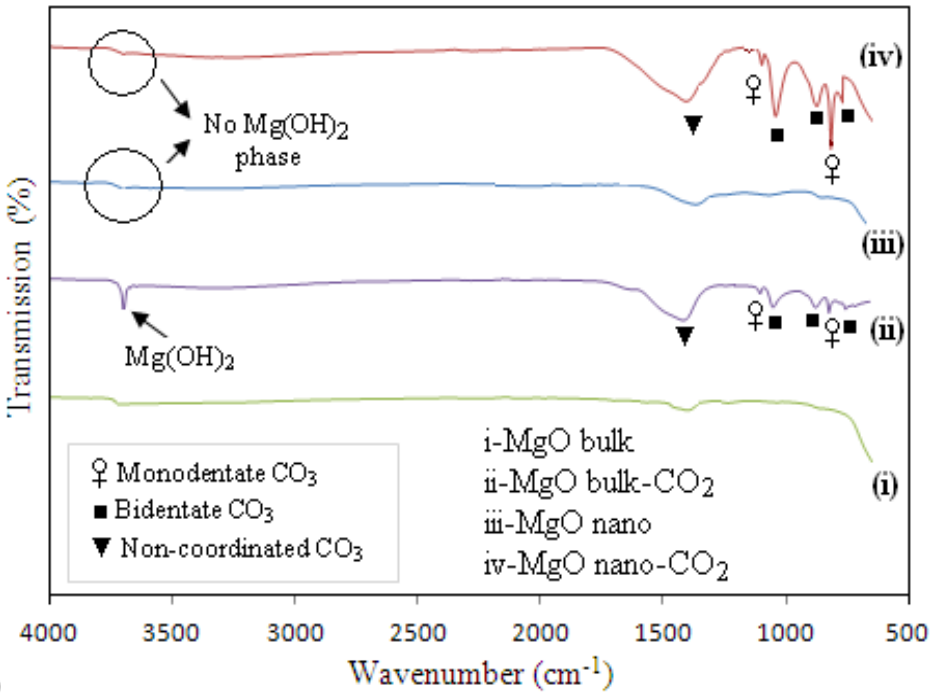

(a)

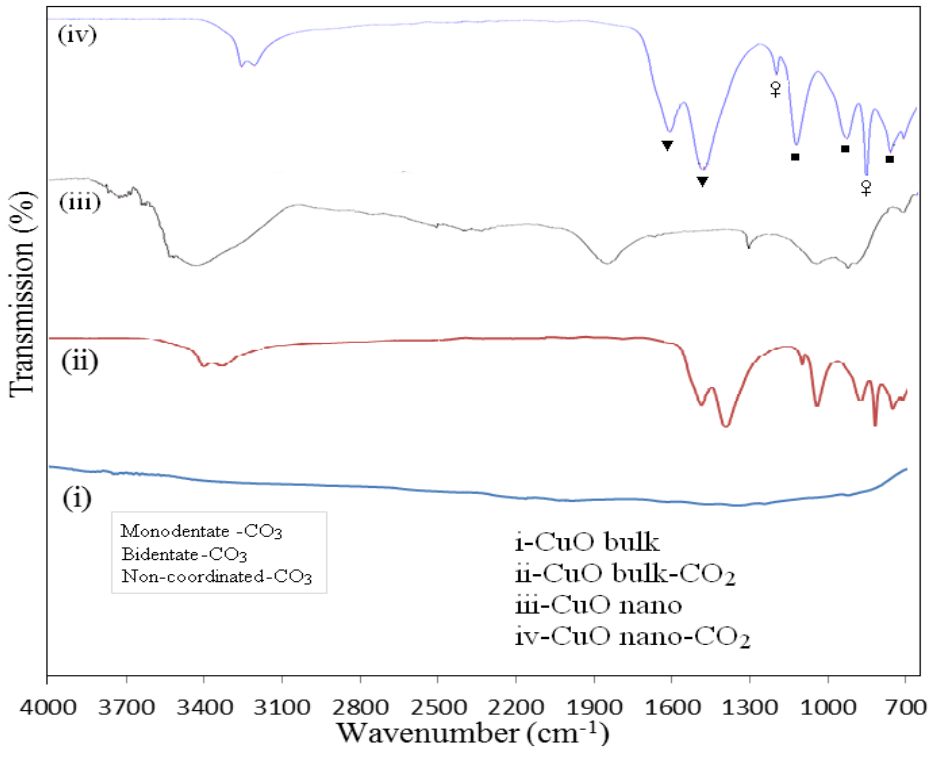

Figure 2. FT-IR spectra of (a) MgO; (i) bulk (ii) bulk-CO_2, (iii) nanoparticle, (iv) nanoparticle-CO_2 (b) CuO; (i) bulk, (ii) bulk-CO_2, (iii) nanoparticle, and (iv) nanoparticle-CO_2

3.4 Surface Micrographs

The morphology and particle size of the adsorbents were studied thoroughly by TEM analysis. The TEM micrograph in Fig. 3 (a) shows the spherical shape of CuO particles with sizes ranging from 20 to 45 nm. The smaller size of the particles influenced the adsorption by greatly increasing the surface area [17]. Fig. 3 (b) shows that the MgO nanoparticles feature a large number of edges and corners, step edges and top corners, and numerous basic sites of various strength (surface hydroxyl such as $Mg(OH)_2$ and low-coordinated O_2 sites), which are recognized as active sites in heterogeneous catalysis [19]. Indeed, these results were also in good agreement with the XRD results. The size of MgO nanoparticles ranged from 25 to 50 nm.

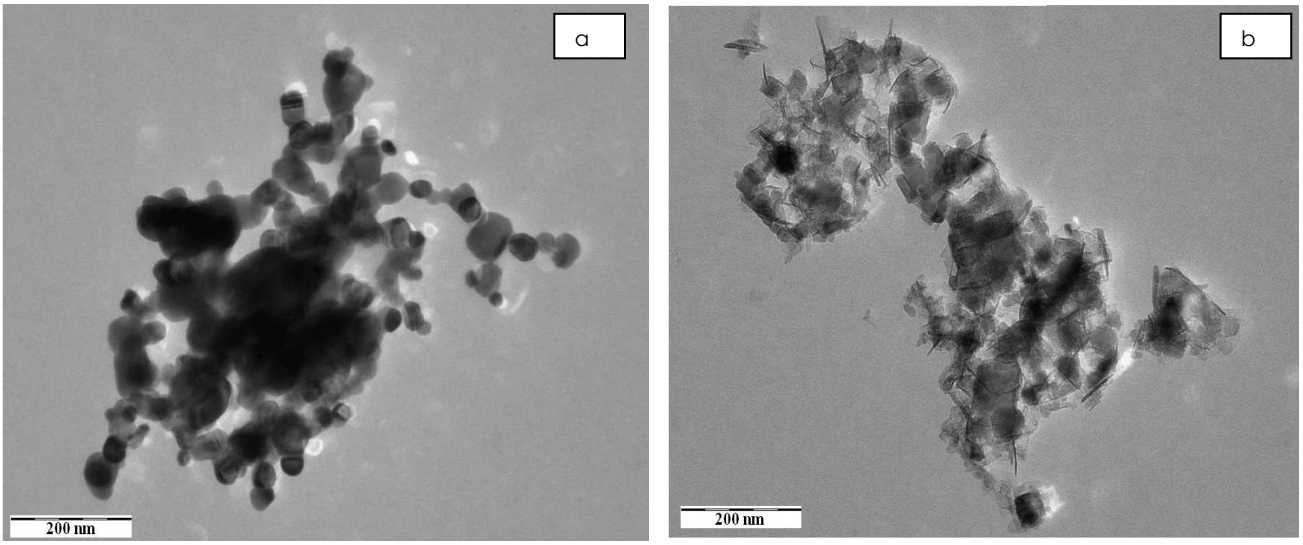

Figure 3. Surfaces micrograph for (a) CuO nanoparticles, (b) MgO nanoparticles

3.5 Quantitative Measurements of CO_2 Adsorption

From the TGA graph in Fig. 4 (a), there is a reduction of 20.1 wt%. The reduction was recorded from 190 °C to 700 °C, corresponding to the decomposition of $CuCO_3$ into CuO. Even though the adsorption process was carried out at room temperature and pressure, the CO_2 adsorption ability of CuO seems to be quite good. The reactions involved are as follows.

$$CuO + CO_2 \rightarrow CuCO_3 \qquad \Delta H_r = -45.5 \text{ kJ·mol}^{-1}$$

Meanwhile, the TGA analysis of the MgO nanoparticles in Fig. 4 (b) showed a relatively high weight decrease of 60.8 wt%, which represents to the amount of adsorbed CO_2. From the weight reduction, it was assumed that 60.8% of the MgO nanoparticles were successfully converted into $MgCO_3$ at room temperature and pressure. This may be due to the formation of CO_2 multilayers and monolayers on the MgO surfaces. These results clearly show that the adsorption of CO_2 by MgO nanoparticles is very fast and efficient. The weight change of $MgCO_3$ (which formed after CO_2 adsorption) can be split into three steps. The first two weight losses occur at the temperature ranges 50–130 and 130–380 °C, corresponding to weak CO_2 dissociation and multilayer desorption, respectively. In addition, there are other curves indicating the weight loss of the CO_2 monolayer at a temperature of 400–650 °C. The reaction involved is as follows.

$$MgCO_3 \rightarrow MgO + CO_2 \qquad \Delta H_r = -117.5 \text{ kJ·mol}^{-1}$$

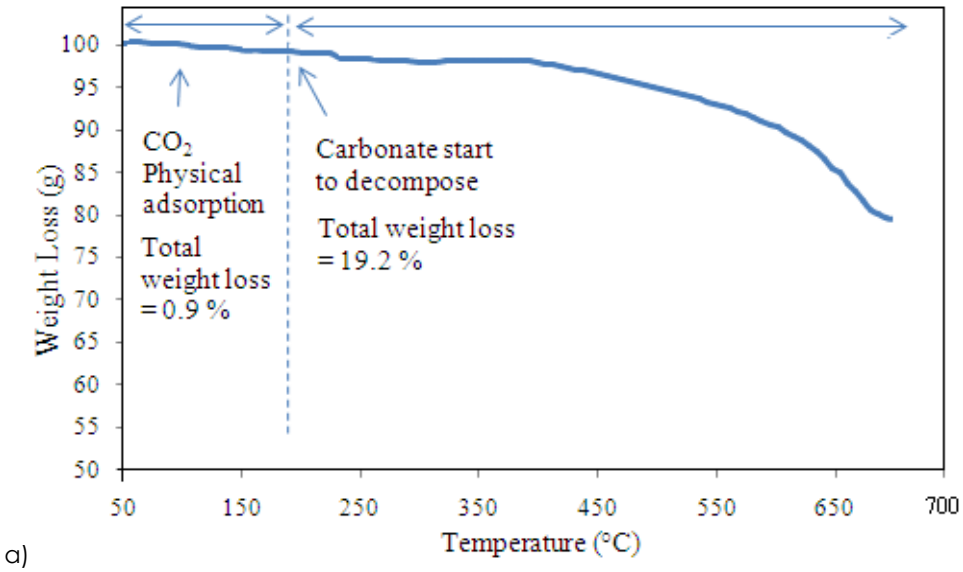

a)

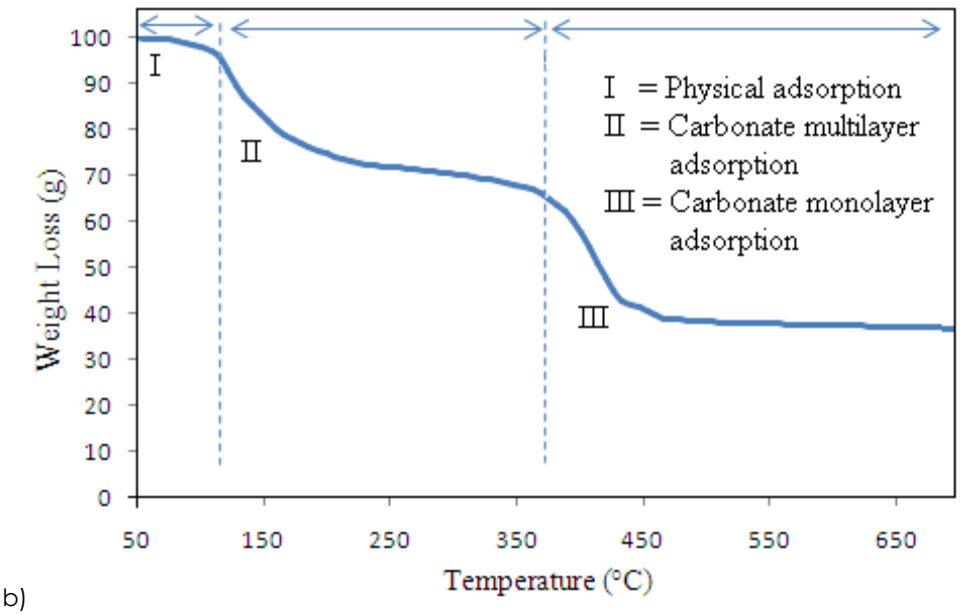

b)

Figure 4 TGA for (a) CuO nanoparticles and (b) MgO nanoparticles

3.6 Effectiveness of Adsorption Process

Generally, CO_2 adsorption phenomena can be divided into two types, namely, physisorption and chemisorption [24]. The physisorption and chemisorption behavior of the metal oxides nanoparticles were studied using CO_2 adsorption isotherm and TPD-CO_2 techniques, respectively, which are discussed below.

a) Physical adsorption

The physical adsorption, or physisorption, of selected adsorbents was determined by Physisorption analysis. By CO_2 adsorption isotherm analysis, it was clearly shown that the MgO nanoparticles showed a higher physical adsorption than bulk MgO, with a value close to 20 cm^3/g (Fig. 5). This value was also higher that for the CuO nanoparticles and bulk CuO. This may be due to the higher surface area of the MgO nanoparticle, which increases the interaction ability of CO_2 and surfaces. The high surface area was confirmed by BET analysis, as previously discussed in Table 2. The basic sites which favor reversible CO_2 physisorption participate as shown below.

$$Mg\text{-}O + CO_2 \rightarrow Mg\text{-}O\cdots CO_2 \text{ (phys. ad)}$$

b) Chemical interactions

The chemical interaction between CO_2 and metal oxide was studied by TPD-CO_2. This method measured the adsorption of CO_2 with increasing temperature. In Fig. 6 (a), one peak was detected at 250 °C, which corresponded to the low chemical adsorption on the MgO mesoporous structure. Another two peaks shown at relatively higher temperatures of 380 and 425 °C represent the higher chemical attraction force of CO_2 with adsorbent surface due to higher basicity levels. The total amount of CO_2 desorbed from the MgO nanoparticles was 5.0 mmol/g. Previous reports suggest that such high CO_2 desorption is possible only through the chemisorption of CO_2 molecules by the metal oxide [25-27].

For the CuO nanoparticles, there was only one clear peak, which represented –CO_2 chemisorption, at 248 °C (Fig. 6 (b)). The large amount of surface active sites of the MgO or CuO nanoparticles initially holds the CO_2 molecules with a smaller affinity, and they are then trapped into the pores by the chemical reaction of MgO or CuO and CO_2 to form $MgCO_3$ or $CuCO_3$. The chemisorptions of CO_2 to form $MgCO_3$ or $CuCO_3$ is supported by the XRD results, which show the characteristic peaks of $MgCO_3$, as discussed in sub-section 3.2.

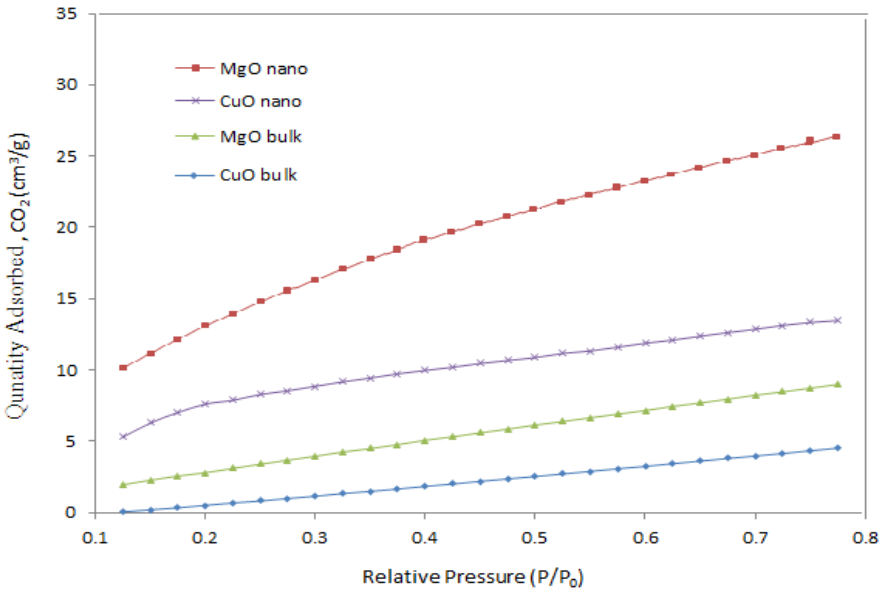

Figure 5 Physical adsorption of CuO and MgO bulk and nanoparticles

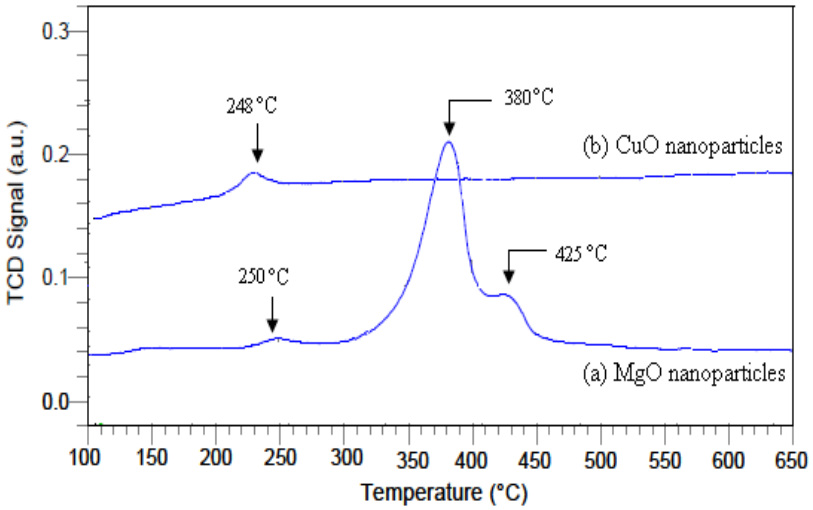

Figure 6 Chemical interaction studies of (a) MgO and (b) CuO nanoparticles with CO_2

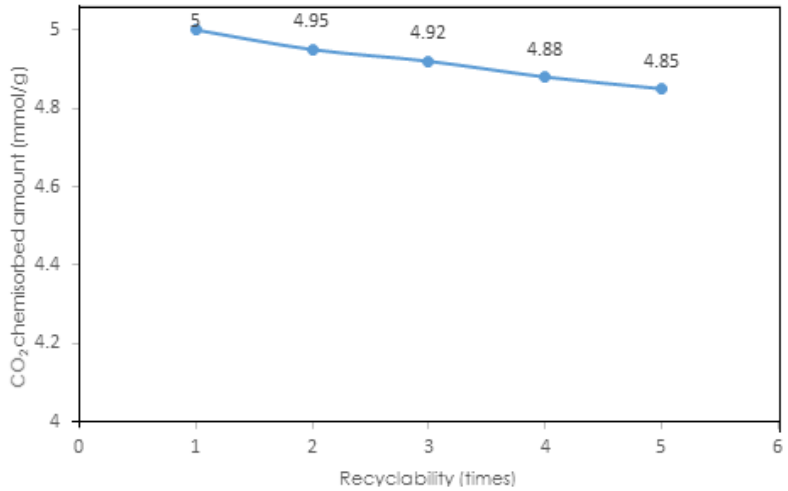

Figure 7 Effect of recyclability to CO_2 chemisorption behavior of MgO nanoparticles

c) Recyclability of adsorbents

The recyclability of the MgO nanoparticles was examined because of their higher CO_2 capture ability compared to the CuO nanoparticles. For the fresh MgO nanoparticles, 5.0 mmol/g of CO_2 chemisorption was measured at 40 °C. After the fifth cycle, no significant loss of the CO_2 adsorption ability was found; was only 3% reduction (from 5.0 mmol/g to 4.85 mmol/g) in the chemisorption ability was observed, as shown in Fig. 7. This slight reduction was probably due to some agglomeration caused by sintering phenomena that occurred in the nanoparticles during the thermal desorption. Subsequently, the surface area of used nano-MgO was slightly decreasing after 5 times recycle.

4.0 CONCLUSIONS

This paper reports the complete physical and chemical interactions of CO_2 on CuO and MgO nanoparticle surfaces. The results showed that MgO nanoparticles show a better adsorption behavior compared with CuO nanoparticles and bulk MgO and CuO. From the TGA studies, the MgO nanoparticles showed a mass loss of 60.8 wt%, which is explained by the chemical interaction of CO_2 with MgO particles or surfaces that results in multilayer adsorption. From the TPD-CO_2 analysis, it is clear that chemical interactions that form $MgCO_3$ were deconvoluted into two peaks representing different species of adsorbed CO_2. The amount of CO_2 adsorption through chemisorption is 5.0 mmol/g.

Acknowledgement

The authors wish to thank Universiti Kebangsaan Malaysia (UKM) for funding this project under research grant, GGPM-2015-014, DPP-2015-FKAB and Long Term Research Grant (LRGS/BU/2011/USM-UKM/PG/02) from the Ministry of Education (MOE) Malaysia and the Centre of Research and Innovation

Management (CRIM) UKM for the use of the instruments.

References

[1] Stewart, C. and M. Hessami. 2005. A Study Of Methods Of CO_2 Capture And Sequestration - The Sustainability Of A Photosyntetic Bioreactor Approach. *Energy Conversion & Management.* 46: 403-420.

[2] Yang, H. Q., Z. H. Xu., M. H. Fan., R. Gupta., R. B. Slimane., A. E. Bland, and I. Wright. 2008. Progress in CO_2 Separation And Capture: A Review. *Journal of Environmental Science. 20*: 14-27.

[3] The Annual Energy Outlook 2013 (AEO2013) was prepared by the U.S. Energy Information Administration (EIA). April 2013.

[4] Isahak, W. N. R. W., M. W. M. Hisham., M. A. Yarmo and Y. H. Taufiq-Yap. 2012. A Review On Bio-Oil Production From Biomass By Using Pyrolysis Method. *Renewable & Sustainable Energy Reviews.* 16: 5910-5923.

[5] Ramesh, T., S. Su., X. X. Yu., and J. S. Bae. 2013. Application Of Carbon Fibre Composites To CO_2 Capture From Flue Gas. *International Journal of Greenhouse Gas Control. 13*: 191-200.

[6] Isahak, W. N. R. W., M. W. M. Hisham, and M. A. Yarmo. 2013. Highly Porous Carbon Materials From Biomass By Chemical And Carbonization Method: A Comparison Study. *Journal of Chemistry*. *Article ID 620346*, 1-6.

[7] Isahak, W. N. R. W., N. Hamzah., N. A. M. Nordin., M. W. M. Hisham, and M. A. Yarmo. 2013. Dehydration Studies Of Biomass Resources For Activated Carbon Production Using BET And XRD Techniques. *Advanced Materials Research. 620*: 491-495.

[8] Han, K. K., Y. Zhou., Y. Chun, and J. H. Zhu. 2012. Efficient MgO-Based Mesoporous CO_2 Trapper And Its Performance At High Temperature. *Journal of Hazardous Materials*. 203: 341-347.

[9] Almazàn-Almazàn, M. C., J. I. Paredes., M. Perez-Mendoza., M. Domingo-Garcia., I. Fernandez-Morales., A. Martinez-Alonso and F. J. Lopez-Garzon. 2006. Surface Characteristics Of Activated Carbon Obtained By Pyrolysis Of Plasma Pretreated PET. *Journal of Physical Chemistry B*. 110: 11327-11332.

[10] Park, S. J. 1999. In: Hsu, J.P., Editor. Interfacial Forces And Fields: Theory And Applications. New York: MARCEL Dekker.

[11] S Lee, S. C., B. Y. Choi., T. J. Lee., C. K. Ryu., Y. S. Ahn, and J. C. Kim. 2006. *CO_2 Absorption And Regeneration Of Alkali Metal-Based Solid Sorbents*. Catalysis Today. 111: 385-390.

[12] Lee, S. C., H. J. Chae., S. J. Lee., B. Y. Choi., C. K. Yi., J. B. Lee, C. K. Ryu, and J. C. Kim. 2008. Development Of Regenerable MgO-Based Sorbent Promoted With K_2CO_3 For CO_2 Capture At Low Temperatures. *Environmental Science and Technology*. 42: 2736-2741.

[13] Baltrusaitis, J., J. Schuttlefield., E. Zeitler, and V. H. Grassian. 2011. Carbon Dioxide Adsorption On Oxide Nanoparticle Surfaces. *Chemical Engineering Journal.* 170: 471-481.

[14] Abid, H.R., J. Shang., H. M. Ang, and S. Wang. 2013. Amino-Functionalized Zr-MOF Nanoparticles For Adsorption Of CO_2 and CH4. *International Journal of Smart Nano Materials.* 4(1): 72-82.

[15] Baltrusaitis, J. and V. H. Grassian. 2005. Surface Reactions Of Carbon Dioxide At The Adsorbed Water-Iron Oxide Interface. *Journal of Physical Chemistry B. 109*: 12227-12230.

[16] Kim, B. J., K. S. Cho, and S. J. Park. 2010. Copper Oxide-Decorated Porous Carbons For Carbon Dioxide Adsorption Behaviors. *Journal of Colloid Interface Science. 342*: 575-578.

[17] Isahak, W. N. R. W., Z. A. C. Ramli., M. W. Ismail., K. Ismail., M. R. Yusop., M. W. M. Hisham, and M. A. Yarmo. 2013. Adsorption-Desorption Of CO_2 On Different Type Of Copper Oxides Surfaces: Physical And Chemical Attractions Studies. *Journal of CO_2 Utilization. 2*: 8-15.

[18] Wagman, D. D., W. H. Evans, V. B. Parker, R. H. Schumm, I. Halow, S. M. Bailey, K. L. Churney, R. L. Nutall, 1989. The NBS Tables of Chemical Thermodynamic Properties Selected Values For Inorganic And C1 C2 Organic Substance In SI Units. *Journal of Physical Chemistry Reference Data.* 18: 1807.

[19] Isahak, W. N. R. W., Z. A. C. Ramli., M. W. M. Hisham, and M. A. Yarmo. 2013. Magnesium Oxide Nanoparticles On Green Activated Carbon As Efficient CO_2 Adsorbent. *AIP Conference Proceedings. 1571*: 882-887.

[20] Isahak, W. N. R. W., M. Ismail., J. M. Jahim., J. Salimon, and M. A. Yarmo. 2012. Characterisation And Performance Of Three Promising Heterogeneous Catalysts In Transesterification Of Palm Oil. *Chemical Papers. 66*: 179-187.

[21] Isahak, W. N. R. W., M. Ismail., N. M. Nordin., N. F. Adnan., J. M. Jahim., J. Salimon, and M. A. Yarmo. 2012. Selective Synthesis Of Glycerol Monoester With Heteropoly Acid As A New Catalyst. *Advanced Materials Research. 545*: 373-378.

[22] Freund, H. J. and M. W. Roberts. 1996. Surface chemistry of carbon dioxide. *Surface Science Reports. 25*: 225-273.

[23] Kuhlenbeck, H., C. Xu., B. Dillmann., M. Habel., B. Adam., D. Ehrlich., S. Wohlrab., H. J. Freund., U. A. Ditzinger., H. Neddermeyer., M. Neumann, and M. Neuber. 1992. Adsorption And Reaction On Oxide Surfaces: CO and CO_2 On Cr_2O_3 (111). *Berichte der Bunsengesellschaft für Physikalische Chemie*. 96: 15-27.

[24] Atkins, P., & De Paula, P. 2010. *Atkins Physical Chemistry*. *9th* edition. Freeman, W.H. and Company. Oxford University Press, New York.

[25] Bhagiyalakshmi, M., Ji, Y. L., & Hyun, T. J. 2010. Synthesis Of Mesoporous Magnesium Oxide: Its Application To CO_2 Chemisorption. *International Journal of Greenhouse Gas Control.* 4: 51-56.

[26] Ram Reddy, M. K., Xu, Z. P., & Diniz da Costa, J. C. 2008. Influence Of Water On High Temperature CO_2 Capture Using Layered Double Hydrocide Derivatives. *Industrial and Engineering Chemistry Research.* 47: 2630-2635.

[27] Isahak, W.N.R.W., Ramli, Z.A.C., Hisham, M.W.M., Yarmo, M.A. 2015. *Renewable and Sustainable Energy Reviews.* 47: 93.